LBL-33511
UC-404
Preprint

Lawrence Berkeley Laboratory
UNIVERSITY OF CALIFORNIA

Materials Sciences Division

Submitted to Brazilian Journal of Physics

Optical Properties of Magnetic Surfaces, Interfaces, Thin Films, Overlayers, and Superlattices

L.M. Falicov

January 1993

REFERENCE COPY
Does Not
Circulate
Bldg. 50 Library.
LBL-33511
Copy 1

Prepared for the U.S. Department of Energy under Contract Number DE-AC03-76SF00098

DISCLAIMER

This document was prepared as an account of work sponsored by the United States Government. Neither the United States Government nor any agency thereof, nor The Regents of the University of California, nor any of their employees, makes any warranty, express or implied, or assumes any legal liability or responsibility for the accuracy, completeness, or usefulness of any information, apparatus, product, or process disclosed, or represents that its use would not infringe privately owned rights. Reference herein to any specific commercial product, process, or service by its trade name, trademark, manufacturer, or otherwise, does not necessarily constitute or imply its endorsement, recommendation, or favoring by the United States Government or any agency thereof, or The Regents of the University of California. The views and opinions of authors expressed herein do not necessarily state or reflect those of the United States Government or any agency thereof or The Regents of the University of California and shall not be used for advertising or product endorsement purposes.

Lawrence Berkeley Laboratory is an equal opportunity employer.

DISCLAIMER

This document was prepared as an account of work sponsored by the United States Government. While this document is believed to contain correct information, neither the United States Government nor any agency thereof, nor the Regents of the University of California, nor any of their employees, makes any warranty, express or implied, or assumes any legal responsibility for the accuracy, completeness, or usefulness of any information, apparatus, product, or process disclosed, or represents that its use would not infringe privately owned rights. Reference herein to any specific commercial product, process, or service by its trade name, trademark, manufacturer, or otherwise, does not necessarily constitute or imply its endorsement, recommendation, or favoring by the United States Government or any agency thereof, or the Regents of the University of California. The views and opinions of authors expressed herein do not necessarily state or reflect those of the United States Government or any agency thereof or the Regents of the University of California.

LBL-33511

OPTICAL PROPERTIES OF MAGNETIC SURFACES, INTERFACES, THIN FILMS, OVERLAYERS, AND SUPERLATTICES*

L. M. Falicov

Department of Physics
University of California
Berkeley, CA 94720

and

Materials Sciences Division
Lawrence Berkeley Laboratory
Berkeley, CA 94720

January 1993

*This work was supported in part by the Director, Office of Energy Research, Office of Basic Energy Sciences, Materials Sciences Division of the U. S. Department of Energy under Contract No. DE-AC03-76SF00098.

Printed on recycled paper

Optical Properties of Magnetic Surfaces, Interfaces, Thin Films, Overlayers, and Superlattices

L. M. Falicov

Department of Physics,

University of California,

Berkeley, CA 94720

and

Materials Sciences Division,

Lawrence Berkeley Laboratory,

Berkeley, CA 94720

ABSTRACT

A brief general review of the optical properties of magnetic surfaces, interfaces, thin films, overlayers, and superlattices is presented. It includes general background material, and some of the latest developments in the field.

January 29, 1993

Optical Properties of Magnetic Surfaces, Interfaces, Thin Films, Overlayers, and Superlattices

L. M. Falicov

Department of Physics,

University of California,

Berkeley, CA 94720

and

Materials Sciences Division,

Lawrence Berkeley Laboratory,

Berkeley, CA 94720

1. INTRODUCTION

Magnetism is an electronically driven phenomenon, and therefore susceptible to study by optical means. It is however a weak phenomenon, as compared with electrostatic and electric-dipole effects, and much more difficult to detect. It is also very subtle in its manifestations. It origins are purely quantum mechanical, with its foundations in the Pauli Exclusion Principle and the existence of the electron spin. It leads nonetheless to short- and long-range forces, and to both classical and quantum-mechanical effects. As a consequence there is a rich variety of textures and properties found in magnetic systems.

It is also possible to alter these systems drastically by means of small changes in temperature, by changes in the specific chemistry and morphology of the samples, and

by relatively modest forces, such as those arising from magnetic fields, and uniform and non-uniform stresses. Therefore magnetic systems lead to a large number of useful engineering and technical applications.[1–5]

2. MAGNETO-OPTICS

The first magneto-optic effect was reported by Faraday in the middle of the XIX century. He discovered that (in general) elliptically polarized light passing through a magnetized, transparent substance (i) changes the ellipticity and (ii) rotates the major axes of its polarization.

About 30 years later, in 1876, Kerr reported an analogous phenomenon in reflection. The Kerr effect is observable in the majority of ferromagnets, which are seldom transparent and therefore not suitable for the Faraday effect. In fact Kerr only reported a rotation in the plane of polarization, but did not notice that there was also a change in the ellipticity of the reflected light. Kerr's explanation of the effect was that the magnetization of the ferromagnet gives rise to a component of the electric-field vector of the light which oscillates in a direction perpendicular to the plane of vibration of the incident beam (and in phase with it). If the incoming light is polarized in the plane of incidence (p-polarization), the reflected light has its strong component in the same plane because of the laws of ordinary reflection. However there is another component, in the reflected beam, polarized in the plane of the surface (s-polarization), perpendicular to the first one. If, as Kerr assumed, the two components are in phase, simple vector addition would give a polarization which is also linear, but with a polarization direction rotated by an angle Θ (the Kerr angle) from the p-direction. In fact the two components *are not in phase,* and the reflected light is thus elliptically polarized. In a typical experiment the main axis of the ellipse is rotated by a few minutes of arc from the original orientation (of the order of 10 minutes for the longitudinal Kerr effect, and about 40 minutes for the polar Kerr effect), and the ellipticity (ratio of the minor to the major axis of the ellipse for light originally linearly p-polarized) is of the

order of 0.001. These are all very small but easily detectable effects.

Given that there are many vectors involved in the problem, the possible geometrical arrangements of the experiment are many. In particular the following vectors are relevant:

Incident light:

Propagation vector **k**;

Instantaneous polarization vector ε perpendicular to **k**.

Reflected light:

Propagation vector $\mathbf{k}'$;

Instantaneous polarization vector ε' perpendicular to $\mathbf{k}'$.

Reflecting magnetic surface:

Unit vector normal to the surface **n**;

Direction of the magnetization **M**.

According to the elementary laws of reflection, **k**, $\mathbf{k}'$ and **n** are all three in one plane, the plane of incidence:

because of the laws of reflection **n** is always parallel to $(\mathbf{k}' - \mathbf{k})$,

because of the laws of reflection **n** is always perpendicular to $(\mathbf{k}' + \mathbf{k})$.

The *Polar Kerr Effect* corresponds to the case in which **M** is parallel to **n**, *i.e.*, the magnetization is normal to the surface and also in the plane of incidence:

POLAR KERR EFFECT: **M** lies parallel to **n**.

In the *Longitudinal Kerr Effect* the magnetization **M** is perpendicular to **n** (*i.e.*, it lies in the surface plane) and is in the plane of incidence:

LONGITUDINAL KERR EFFECT: **M** lies perpendicular to **n** ,

LONGITUDINAL KERR EFFECT: **M** lies parallel to $(\mathbf{k}' + \mathbf{k})$.

In the *Transverse Kerr Effect* the magnetization is once again perpendicular to **n** (*i.e.*, it also lies in the surface plane) and is also perpendicular to the plane of

incidence:

TRANSVERSE KERR EFFECT: **M** lies perpendicular to **n** ,

TRANSVERSE KERR EFFECT: **M** lies perpendicular to (**k**′ + **k**).

All these arrangements are shown in Figure 1.

Since the interaction between electric and magnetic fields is largest when the two vectors are perpendicular to each other, the Kerr rotation is maximum whenever ε and **M** are perpendicular to one another (*e.g.*, the polar and longitudinal effects for *s*-polarization), sizeable when they form a not-very-small angle, and negligible when ε and **M** are parallel or almost parallel.

Even though both magneto-optic effects (Faraday and Kerr) were fist discovered and studied in the second half of the XIX century, they are both now enjoying a renaissance as tools in basic and applied research. On the basic-research side it has been recently demonstrated that the Kerr effect can be used to detect monolayer and even submonolayer magnetism.[6] In the applications area the effects can be useful in connection with the commercial potential of materials for high-density magneto-optical data storage.[7] In addition, recent developments in Kerr microscopy to image magnetic domains and to observe magnetic-switching phenomena has also helped revitalize the classic field of micromagnetics.[8,9]

The Surface Magneto-Optic Kerr Effect (SMOKE) provides a valuable *in situ* characterization probe of the magnetic and magneto-optic properties of magnetic films during the growth process.[10] Since the magneto-optic coupling is caused by the spin-orbit interaction it is indeed a very small effect. The technique requires the application of an external magnetic field to reverse the magnetization direction of the sample in the growth chambers. All other parts, including the optical components, are outside the vacuum system. Typically the system consists of a laser source, a polarizing analyzer, and a photodiode detector (see Figure 2). Magnetic hysteresis curves are obtained by monitoring the light intensity at the detector as the field is swept. To address key

issues associated with the surface magnetic anisotropy, the field can be in the film plane (longitudinal and transverse Kerr effects) or perpendicular to it (polar Kerr effect). The temperature dependence of the hysteresis loops can be used to monitor the magnetization and coercivity. The Kerr effect was also used to obtain the magnetization exponent β in the critical regime for the system Fe/Pd (100), and a good agreement was found with that expected theoretically ($\beta = 0.125$) for a two-dimensional Ising system[11]. The Kerr effect can be used as well to monitor the Curie temperature as a function of thickness, which provides a fundamental characterization parameter of the films of interest.

It should be possible in the very near future to use tunable photon sources (synchrotron sources) in the optical-frequency region to monitor the Kerr rotation of magnetic monolayers and ultra-thin, metastable phases. This form of the Kerr spectroscopy will provide electronic structural information in the form of a joint density of states weighted by the magneto-optic matrix elements.[12] The spectral information should complement that obtained from **k**-dependent probes of the band structure, such as angle-resolved, spin-polarized photoemission.

It should be emphasized that the Kerr effect is not an inherently surface-sensitive probe. The optical penetration depth in metals is between 100 and 200 Å, and therefore the probe goes many atomic layers into the bulk. The surface sensitivity, necessary to study surface and interface magnetism, is derived from the sample fabrication techniques that create extremely thin epitaxial magnetic films. It is of interest to use complementary techniques with different probing depths to understand coupled magnetic layers, for instance. It should be possible to develop the Kerr effect into such a probe by using non-linear optical processes; surface sensitivity will be obtained by monitoring the Kerr rotation in the Second-Harmonic Generation (SHG) mode.[13,14] The SHG technique has recently gained prominence as an advanced surface-analysis technique.[15]

3. LIGHT-SCATTERING TECHNIQUES

Brillouin light scattering (inelastic light scattering by low-frequency excitation modes with well defined energy and wavevector) has also proven valuable to obtain information about the magnetization, and the exchange and anisotropy constants. The scattering modes (bosonic excitations created and destroyed) in this case are the spin waves (magnons). These studies can be performed *in situ* on overlayers,[16] or as a post-growth characterization tool on superlattice and sandwich structures[17,18] in air or in controlled high- or low-temperature environments. The information obtained is quantitative and cross-correlates well with other techniques, such as ferromagnetic resonance data.[19]

4. ANGLE-RESOLVED PHOTOEMISSION SPECTROSCOPY

Even without resolution of the spin polarization of the emitted electron, angle-resolved photoelectron spectroscopy (ARPES) is a very powerful tool to study the magnetic properties of valence electrons in solids. Peaks in ARPES are produced by direct (vertical) transition, in which the **k**-vectors in the initial (before photon absorption) and final (after photon absorption) electron states are conserved (within a vector of the reciprocal lattice in the crystal). From the measured energy and angle of the emitted electron, and given that the frequency of the radiation is known, one can determine uniquely the energy of the initial state, and the component of its **k**-vector in the plane of the emitter's surface. Since spin-up and spin-down electrons have different band structures in polarized materials, the detection of specific features in the photoemission spectrum -- with well determined energy and surface components of the **k**-vector -- permit comparison with theoretical calculations based on various magnetic structures, the elimination of many non-compatible models, and the determination (in some cases) of the correct structure.

A successful example of the application of this technique is the study of the (100) surface of antiferromagnetic Cr. It was known from theoretical studies[20–22] that the

(100)

free surface of antiferromagnetic Cr should order itself in the form of alternating ferromagnetic planes. The surface outer plane has a magnetic moment considerably enhanced from its bulk value [between (+2.4) and (+3.0) Bohr magnetons, compared with a bulk value of 0.59 Bohr magnetons]. The second layer, which is ferromagnetic but aligned antiparallel to the outer one, has a magnetic moment of about (-1.5) Bohr magnetons; the third layer a moment of (+1.0) Bohr magnetons. Such a strong magnetic structure (which is, on the whole, antiferromagnetic in nature but -- because of only partial compensation between successive layers -- has a net surface magnetization) yields well defined features in the band structure, in particular surface electronic states that are concentrated on either the surface or on the second atomic layer.

Analysis of the ARPES data[23] confirms the existence of two sharp features. Feature 1, at an energy 0.08 eV below the Fermi level, has a **k**-vector whose surface-parallel component lies at the center of the two- dimensional (surface) Brillouin zone; polarization and photon-energy analysis indicates that it originates from states with the so-called Δ_1 symmetry in the bulk. Feature 2, at an energy 0.63 eV below the Fermi level, lies also at the center of the two dimensional surface Brillouin zone, but originates from bulk states with Δ_5 symmetry. These features can be put in a one-to-one correspondence to those predicted by theory.[20–22] It is highly unlikely that any other magnetic structure could give rise to features which would also agree that well with the experimental data.

Only recently, however, has the ferromagnetic character of the (100) surface of antiferromagnetic chromium been observed directly. The difficulty with the direct observation is the existence, in all real surfaces, of *surface steps*. With each step, one monolayer in height, a different terrace is exhibited. Since alternating terraces have opposite magnetizations (a consequence of the antiferromagnetic arrangement of bulk Cr), there is in fact no net magnetization at the stepped surface. The effect was

nonetheless observed by means of a double Scanning Tunneling Microscopy (STM) experiment.[24] When a (100) chromium surface was observed with an STM with a tungsten tip, many identical steps (all of 1.4 Å height) were recorded. The height corresponds exactly to one half of the 2.8 Å of the cubic parameter in body-centered chromium. A second experiment, in which the tip was made of chromium dioxide (a magnetic semimetal in which only one spin orientation can tunnel either in or out), produced alternating steps of 1.2 Å and 1.6 Å height, proving that for electrons of a given spin (those that can tunnel in or out of the chromium dioxide tip) consecutive terraces present different tunneling probabilities, *i.e.*, terraces with alternating ferromagnetic arrangements.

5. SPIN-POLARIZED PHOTOEMISSION SPECTROSCOPY

Direct information on the ferromagnetic electronic structure at surfaces can be obtained by means of spin-polarized photoemission studies. Early studies[25] measure the polarization of the photo-yield as a function of photon energy, without energy analysis. Such measurements have the advantage that they can be performed as a function of applied magnetic field perpendicular to the surface up to the magnetic saturation of the sample.

Synchrotron radiation, with its high intensity, permits energy analysis of the electrons photoemitted from a material magnetized in the plane of the surface.[26] A movable spin and energy analyzer allows investigation along different directions of **k**-space. One can thus obtain a complete mapping of the spin-dependent electronic band structure over the entire Brillouin zone.[27]

With high-intensity vacuum ultra-violet and soft x-ray sources other investigations become possible. Studies of surface shifts in shallow core levels, such as the $4f$ levels in rare earths, allow one to distinguish varying magnetization as the surface is approached.[28] With x-ray photoemission spectroscopy the polarization of electrons emitted from multiplet split core levels, such as the $3s$ or $3p$ level in Fe, gives

element-specific magnetic information,[29] similar to that obtained from polarized Auger spectroscopy but easier to interpret. From these studies it is also possible to extract quantitative values of atomic magnetic moments at surfaces.[30]

6. POLARIZED AUGER SPECTROSCOPY

Auger electron spectroscopy is a powerful tool for surface analysis because of its surface sensitivity and its chemical-element specificity. In the case of ferromagnets the Auger electrons may also be spin polarized. Such polarization arises from the different occupation of the spin-split valence- conduction band. When the electrons at the top of the Fermi distribution in a ferromagnet are directly involved in the Auger emission process, the emitted electrons are naturally polarized. For core electrons, on the other hand, there also may be polarized emission because of the exchange interaction between the valence-electron spin density and the filled core levels.

Through spin-polarized Auger spectroscopy one obtains an element- specific probe of the local magnetization at a given site. It can provide information not only on the magnetic properties of a surface but, in films of a few atomic layers, on the magnetic properties of substrates and interfaces.

A classic study of this kind[31] has determined univocally the magnetization of a monolayer of Gd evaporated on an Fe(100) crystal surface. The spin polarization of the Auger electrons corresponding to the Fe [$M(23)M(45)M(45)$] line has opposite polarization to that corresponding to the Gd [$N(45)O(23)N(67)$] and Gd [$N(45)N(67)N(67)$] lines, indicating that the magnetic moments in the Gd overlayer are coupled so as to lie in a direction antiparallel to those in the Fe substrate. In the same study it was possible to measure independently the temperature dependence of the magnetization of the Gd layer and the Fe interface layers taking advantage of the elemental specificity of the Auger process.

7. MAGNETIC SUPERLATTICES

Metallic magnetic superlattices[1] are made by depositing, in an orderly fashion and with clean interfaces, alternating metallic thin films of two or more chemical compositions, at least one of which is magnetic. These systems exhibit a wide range of very interesting new physical phenomena, in particular magneto-optics, magnetoresistance, magnetostriction, magnetostatics, magnetic exchange coupling, unusual microwave properties, and anisotropic magnetic behavior.

A variety of procedures have been used to grow these superlattices. The preferred methods have been sputtering, evaporation, molecular beam epitaxy, and chemical vapor deposition. A typical superlattice consists of a sometimes complex substrate (*e.g.*, gallium arsenide, magnesium oxide, strontium titanate, copper, molybdenum), followed by a repetition (a given number of times, between one and several hundred) of a thickness x of a ferromagnetic metal (*e.g.*, iron, cobalt, permalloy) and a thickness y of a non-magnetic metal (*e.g.*, copper, chromium, molybdenum). The non-magnetic metal is usually called the spacer. Two closely related effects appear in these systems:

1.- Successive ferromagnetic layers arrange themselves with their magnetization either parallel or antiparallel to each other (see Figure 3). The (parallel or antiparallel) magnetic arrangement is a function of the thickness and nature of the intervening non-ferromagnetic metal and the quality and structure of the interfaces. For a given system, prepared in a systematic way, the coupling is an oscillatory function of the thickness of the spacer[32,33] (see Figures below).

2.- The second effect takes place in samples in which the magnetic alignment is antiparallel. The application of a strong enough magnetic field changes the arrangement of the magnetization. The antiferromagnetic coupling is overcome, and the magnetic moments of all ferromagnetic layers are forced to lie in the same direction. A macroscopic magnetic moment develops. Simultaneously the electrical resistance of the superlattice, in all directions, decreases.

The change in the magnetic structure as a function of the structure of the sample and the applied magnetic field has been monitored by optical (SMOKE, Brillouin scattering) and non-optical (neutron and electron scattering techniques, ferromagnetic resonance) means.

SMOKE experiments provide *in situ* characterization of the samples. By monitoring the the Kerr angle as a function of the applied magnetic field, one determines the hysteresis loops of the various samples (through a derivative property). Samples with parallel arrangement exhibit a simple, single loop, similar to those found in ordinary, bulk ferromagnets. Samples with antiparallel arrangements in the absence of an applied field exhibit a double loop, corresponding to the three possible configuration:

{..., ↑, ↑, ↑, ↑, ...} (for strong magnetic fields up);

{..., ↑, ↓, ↑, ↓, ...} (for weak fields);

and {..., ↓, ↓, ↓, ↓, ...} (for strong magnetic fields down).

(See Figures 4, 5, and 6.)

A prominent technical success of the last three years is the growth of a spacer wedge whose thickness varies continuously across the sample.[34] Typically, its thickness varies between 0 and 20 Å over a distance of 0.5 mm. Such a shallow wedge permits the conversion of rather poor horizontal resolution into vertical resolutions in the atomic scale or even better. Wedge samples have been prepared with a variety of elements under a large variety of growth conditions. It should be noted that on the scale of the wedge, it is in fact a succession of "broad" terraces, each one atomic layer higher than the next (Figure 7).

ACKNOWLEDGMENTS

This research was supported at the Lawrence Berkeley Laboratory, by the Director, Office of Energy Research, Office of Basic Energy Sciences, Material Sciences Division, U.S. Department of Energy, under contract No. DE-AC03-76SF00098.

REFERENCES

1 L. M. Falicov, Physics Today, October 1992, p. 46.

2 R. P. H. Chang and J. M. Poate, Mater. Res. Bull, November 1991, p.63.

3 R. M. White, Physics Today, November 1987, p. 89.

4 L. M. Falicov, D. T. Pierce, S. D. Bader, R. Gronsky, K. B. Hathaway, H. J. Hopster, D. N. Lambeth, S. S. P. Parkin, G. Prinz, M. Salamon, I. K. Schuller, and R. H. Victora, J. Mater. Res. **5** , 1299 (1990).

5 *Magnetic Surfaces, Thin Films, and Multilayers,* edited by S. S. P. Parkin, H. J. Hopster, J. -P. Renard, T. Shinjo, and W. Zinn, Mater. Res. Soc., Pittsburgh (1991).

6 E. R. Moog and S.D. Bader, Superlatt. Microstr. **1** , 543 (1987).

7 See D. S. Bloomberg and G. A. N. Connell in *Magnetic Recording,* Volume II: *Computer Data Storage,* edited by C. D. Mee and E. D. Daniel (McGraw-Hill, New York, 1988).

8 F. Schmidt, W. Rave, and A. Hubert, IEEE Trans. Magn. **MAG-21** , 1596 (1985).

9 D. A. Herman, Jr. and B. E. Argyle, IEEE Trans. Magn. **MAG-22** , 772 (1986).

10 C. Liu, E. R. Moog, and D. D. Bader, Phys. Rev. Lett. **60** , 2422 (1988).

11 C. Liu and D. D. Bader, in *Magnetic Properties of Low-Dimensional Systems II,* edited by L. M. Falicov, F. Mejía-Lira, and J. L. Morán-López (Springer-Verlag, Berlin, 1990), p.22.

12 W. Reim, J. Magn. Magn. Mat. **58** , 1 (1986).

13 W. Hübner and K. H. Bennemann, Phys. Rev. B **40** , 5973 (1989).

14 W. Hübner, Phys. Rev. B **42** , 11553 (1990).

15 Y. R. Shen in *Chemistry and Structure at Interfaces: New Laser and Optical Techniques,* edited by R. B. Hall and A. B. Ellis (Verlag Chemie, Weinheim,

1986), p. 151.

16 B. Hildebrands, P. Baumgart, and G. Güntherodt, Phys. Rev. B **36** , 2450 (1987).

17 M. Grimsditch, A. Malozemoff, and A. Brunsch, Phys. Rev. Lett. **43** , 711 (1979).

18 P. Grünberg, R. Schreiber, Y Pang., M. B. Brodsky and H. Sowers, Phys. Rev. Lett. **57** , 2442 (1986).

19 B. Heinrich, A. S. Arrott, J. F. Cochran, C. Liu, and K. Myrtle, J. Vac. Sci. Technol. **A 4** , 1376 (1986).

20 G. Allan, Surf. Sci. 74, 79 (1978); Phys. Rev. B 19, 4774 (1979); Surf. Sci. Rep. **1** , 121 (1981).

21 C. L. Fu, A. J. Freeman, and T. Oguchi, Phys. Rev. Lett **54** , 2700 (1985); C. L. Fu and A. J. Freeman, Phys. Rev. B **33** , 1755 (1986).

22 R. H. Victora and L. M. Falicov, Phys. Rev. B. **31** , 7335 (1985).

23 L. E. Klebanoff, R. H. Victora, L. M. Falicov, and D. A. Shirley, Phys. Rev. B. **32** , 1997 (1985).

24 R. Wiesendanger, H. -J Güntherodt, G. Güntherodt, R. J. Gambino, and R. Ruf, Phys. Rev. Lett. **65** , 247 (1990).

25 M. Campagna, D. T. Pierce, F. Meier, K. Sattler, and H. C. Siegmann, Adv. Electronics and Electron Phys. **41** , 113 (1976).

26 E. Kisker, K. Schroeder, W. Gudat, and M. Campagna, Phys. Rev. B **31** , 329 (1985).

27 P. D. Johnson, A. Clarke, N. B. Brookes, S. L. Hubert, B. Sinkovic, and N. V. Smith, Phys. Rev. Lett. **61** , 2257 (1988).

28 D. Weller, S. F. Alvarado, W. Gudat, K. Schroeder, and M. Campagna Phys. Rev. Lett. **54** , 1555 (1985).

[29] C. Carbone and E. Kisker, Solid State Commun. **65** , 1107 (1988).

[30] Y. Kakehashi, Phys. Rev. B **31** , 7482 (1985).

[31] M. Taborelli, R. Allenspach, G. Boffa, and M. Landolt, Phys. Rev. Lett. **56** , 2869 (1986).

[32] S. S. P. Parkin, R. Bhadra, and K. P. Roche, Phys. Rev. Lett. **67** , 3598 (1991).

[33] S. S. P. Parkin, Phys. Rev. Lett. **67** , 3598 (1991).

[34] J. Unguris, R. J. Celotta, and D. T. Pierce, Phys. Rev. Lett **67** , 140 (1991), Phys. Rev. Lett. **69** , 1125 (1992).

FIGURE CAPTIONS

Figure 1

The arrangement of the various vectors in the magneto-optic experiments. The various letters indicate: E: the incident beam; R: the reflected beam; T: the transmitted beam; M: the sample magnetization. (a) The Polar Kerr effect; (b) The Longitudinal Kerr effect; (c) The Transverse Kerr effect; (d) The Faraday effect.

Figure 2

Schematic experimental arrangement for the Surface Magneto-Optic Kerr Effect (SMOKE) on a trilayer sample of Fe/Mo/Fe. (Figure courtesy of S. D. Bader.)

Figure 3

Schematic representation of a magnetic superlattice. In (a) successive magnetic layers are arranged with their magnetizations antiparallel to each other; the electrical resistance is high. In (b) there is a parallel magnetization arrangement; the resistance is low. If the application of a magnetic field changes (a) into (b) one obtains a *negative magnetoresistance*.

Figure 4

Ferromagnetic and antiferromagnetic hysteresis loops in trilayer samples of Fe/Mo/Fe, with varying thickness of the Mo spacer. The data were taken with the SMOKE technique. See Figure 2 for the experimental arrangement. (Figure courtesy of S. D. Bader.)

Figure 5

Hysteresis loops measured by SMOKE technique in trilayer samples of Fe/Mo/Fe, as a function of the thickness of the Mo spacer. The data were taken with the SMOKE technique. The parallel (single loop) and antiparallel (double loop) arrangements are an oscillatory function of the thickness. (Figure courtesy of S. D. Bader.)

Figure 6

Oscillations in the switching field, as defined in Figure 4, as a function of the Mo spacer thickness in Fe/Mo/Fe trilayers. Finite switching fields indicate antiparallel arrangement of the two Fe layers. Zero switching fields are an indication of parallel arrangement of the Fe layers. (Figure courtesy of S. D. Bader.)

Figure 7

Exploded schematic view of a wedge sample of an Fe/Cr/Fe trilayer. The arrows in the Fe indicate the direction of magnetization in each domain. There are two domains in the Fe whisker substrate, and many domains in the overlaying (top) Fe film. The coupling between the Fe whisker and the Fe film -- parallel or antiparallel -- is a function of the thickness of the Cr spacer. It is also a function of the roughness of the Fe/Cr interfaces. Note that the vertical and horizontal scales are very different. The actual angle of the whisker was in fact 0.001 degrees. (Figure courtesy of R. J. Celotta and D. T. Pierce. See reference 34)

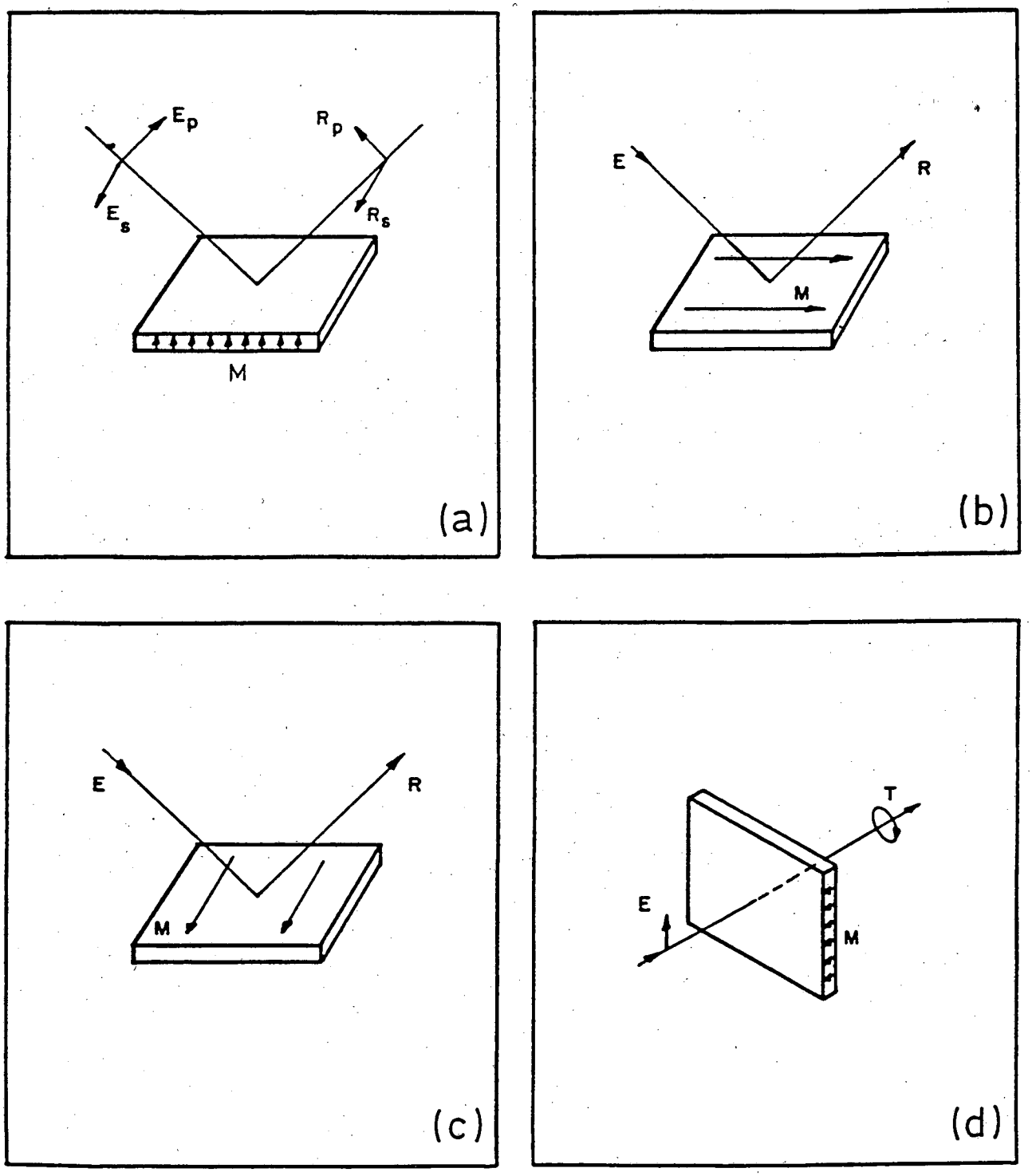

Figure 1

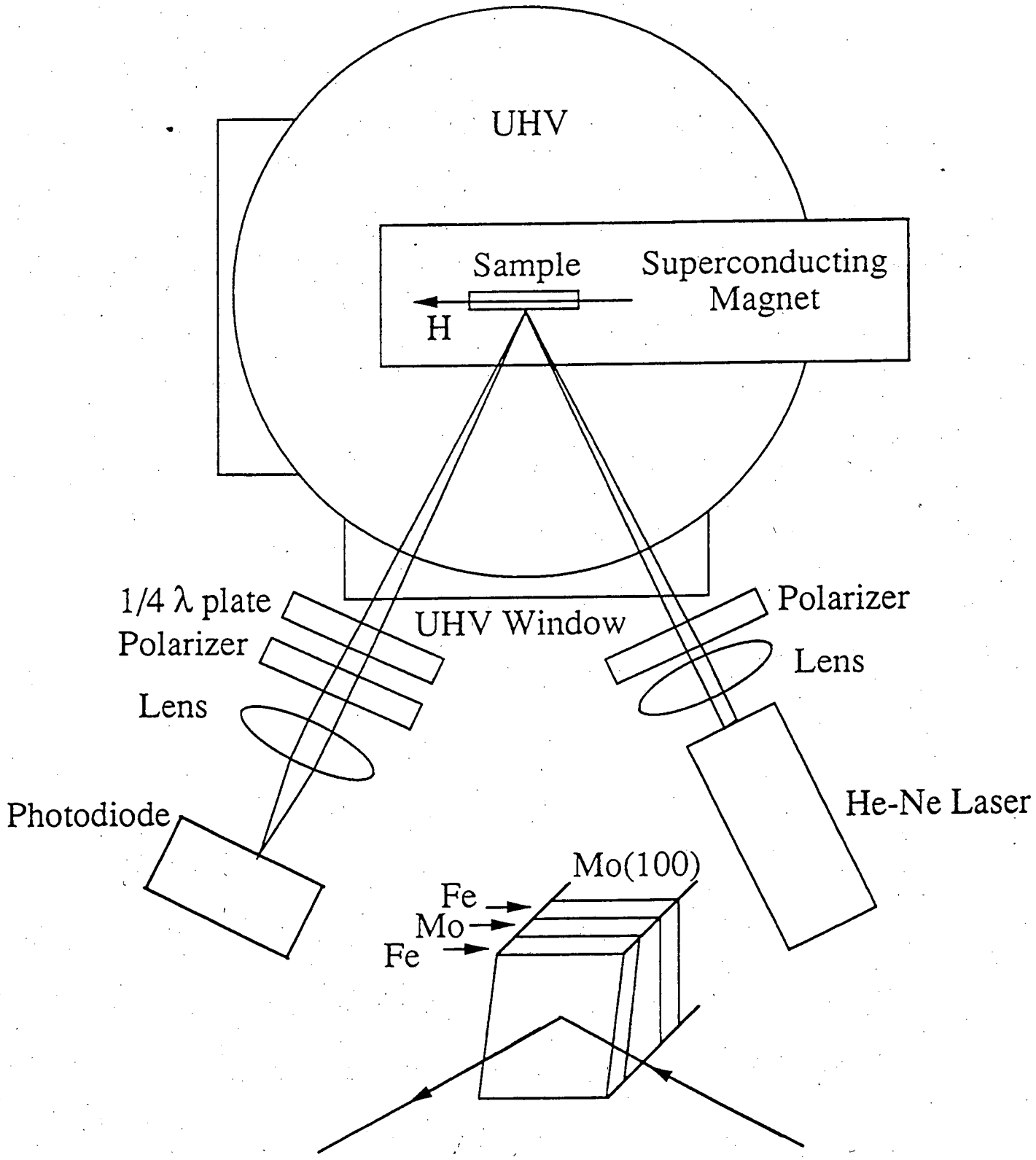
UHV
Sample
Superconducting
Magnet
H
1/4 λ plate
Polarizer
Lens
UHV Window
Polarizer
Lens
Photodiode
He-Ne Laser
Mo(100)
Fe
Mo
Fe

Figure 2

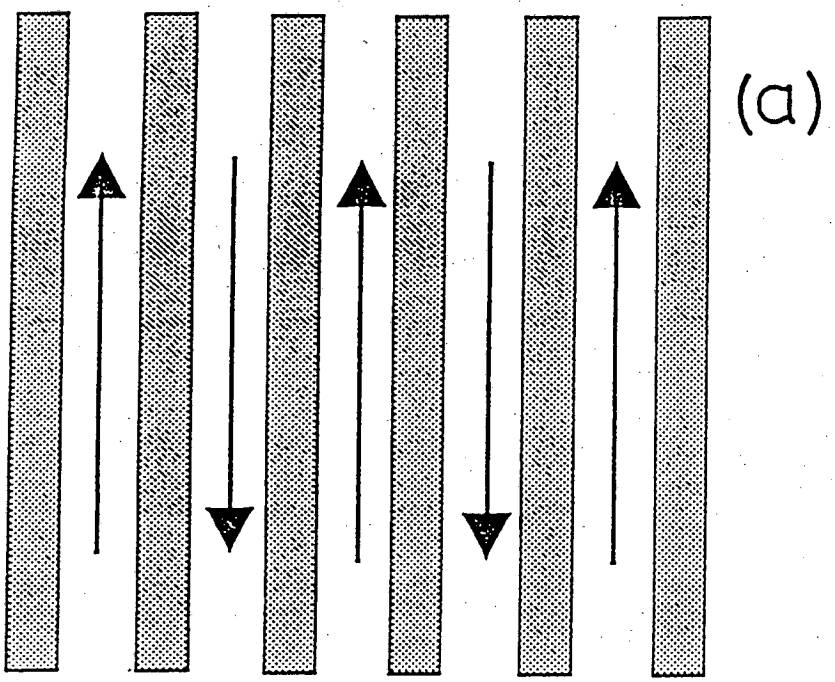

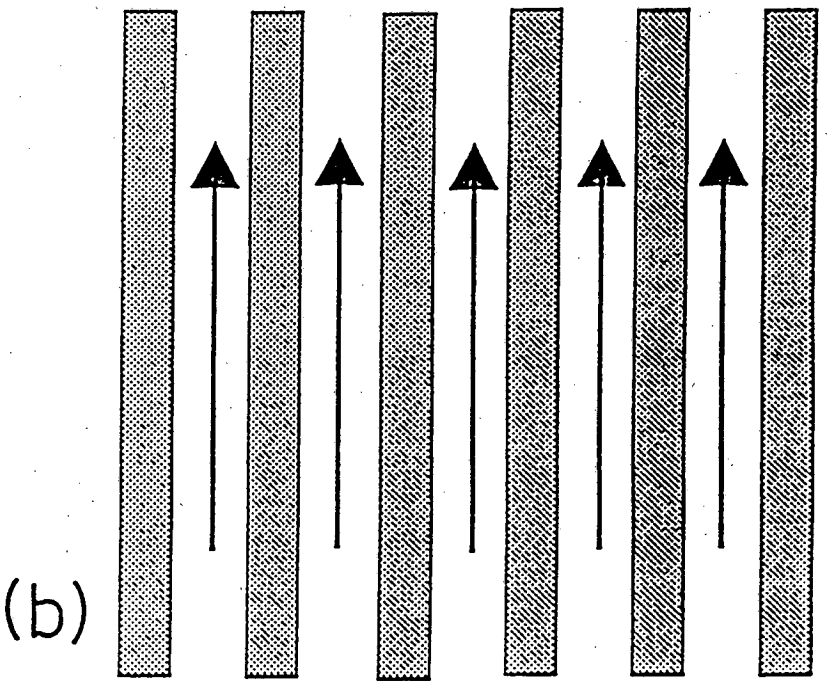

Figure 3

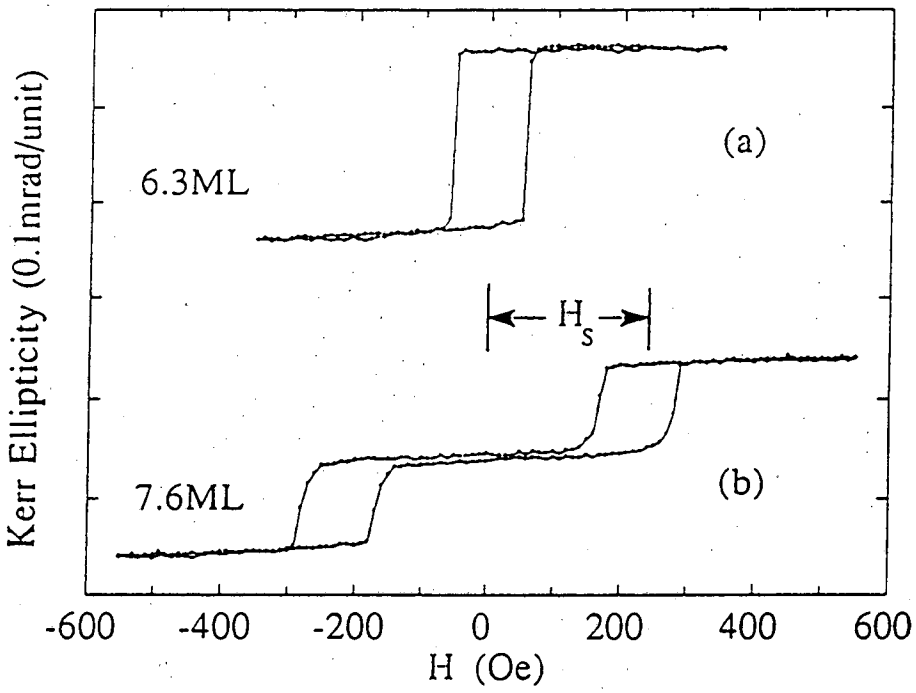
Kerr Ellipticity (0.1mrad/unit)
6.3ML
(a)
H_s
7.6ML
(b)
-600
-400
-200
0
200
400
600
H (Oe)

Figure 4

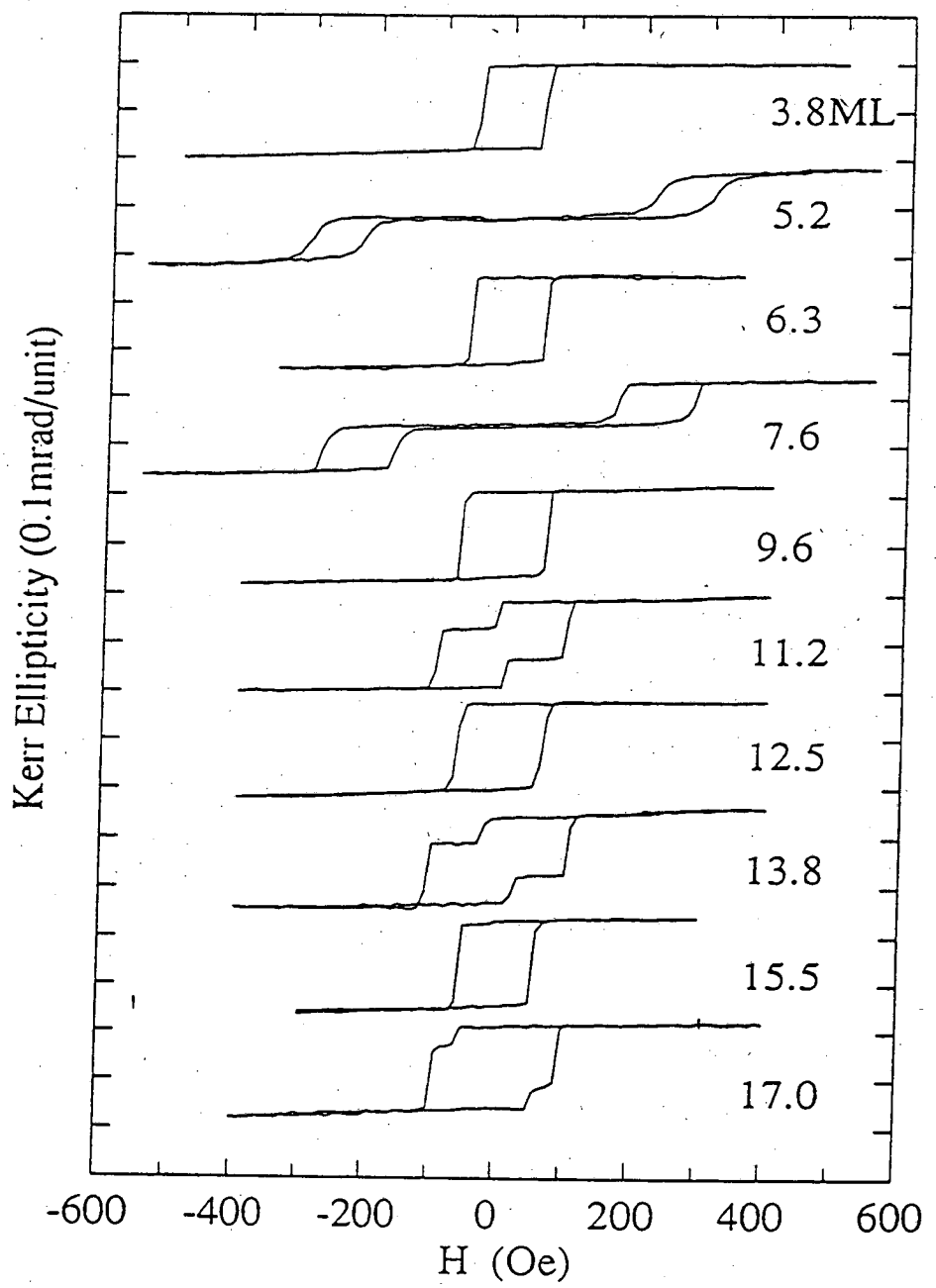
3.8ML
5.2
6.3
7.6
9.6
11.2
12.5
13.8
15.5
17.0
Kerr Ellipticity (0.1mrad/unit)
-600
-400
-200
0
200
400
600
H (Oe)

Figure 5

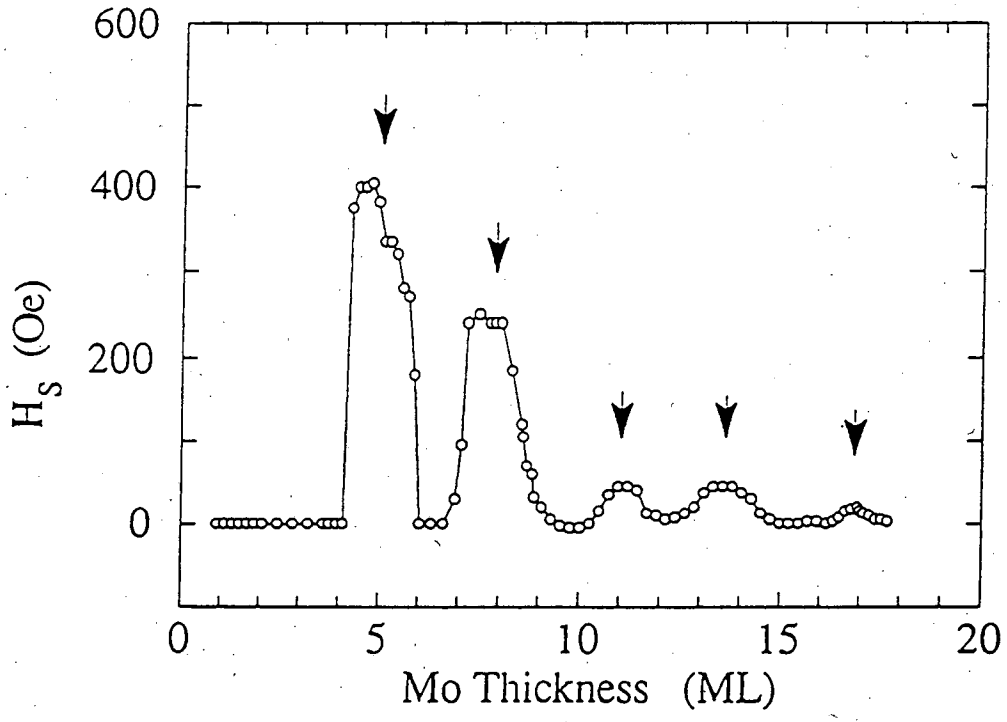

Figure 6

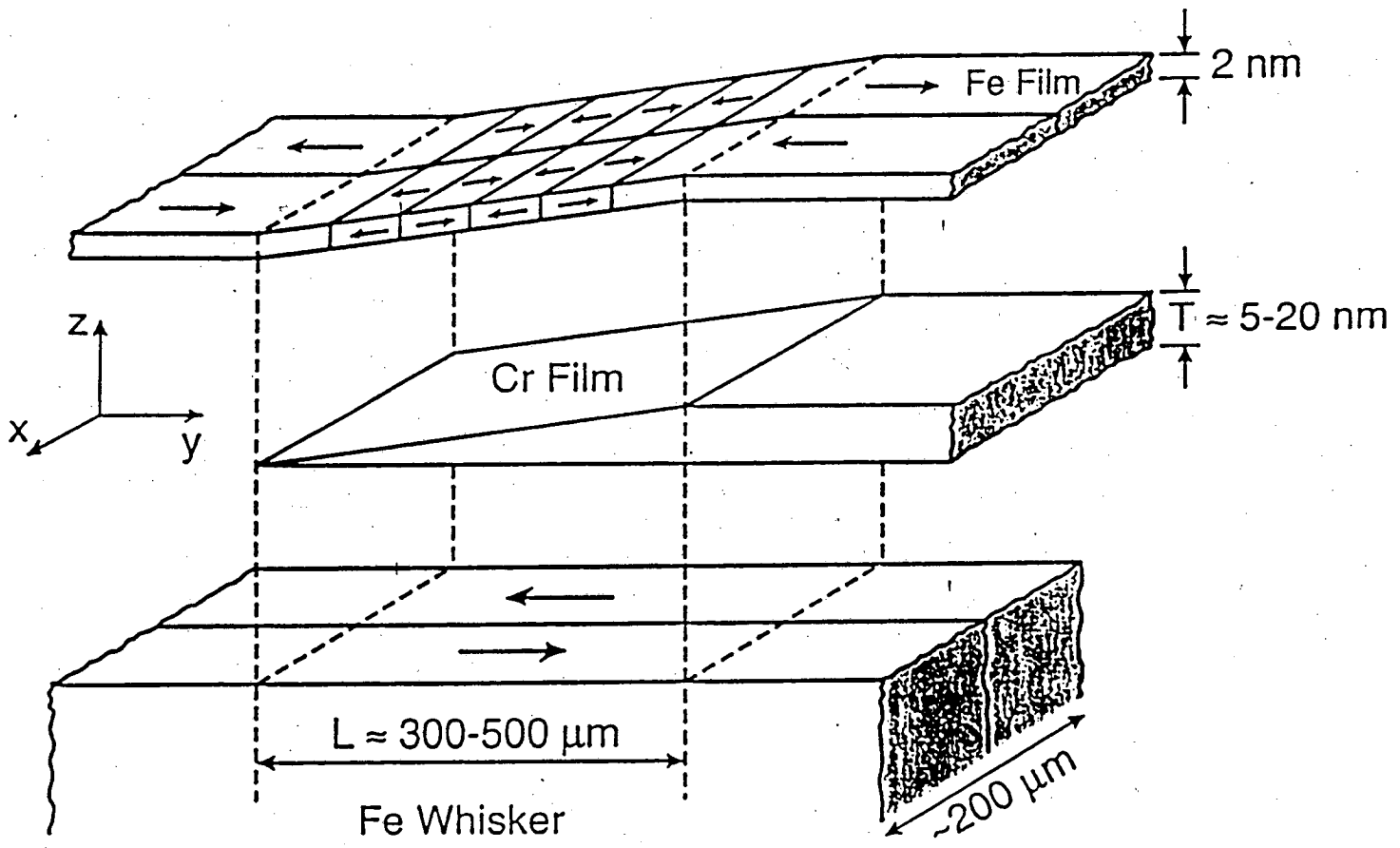

Figure 7

LAWRENCE BERKELEY LABORATORY
UNIVERSITY OF CALIFORNIA
TECHNICAL INFORMATION DEPARTMENT
BERKELEY, CALIFORNIA 94720